www.czasopisma.pan.pl PAN www.journals.pan.pl

ARCHIVES
of
FOUNDRY ENGINEERING

ISSN (2299-2944)
Volume 2020
Issue 4/2020

83 – 90

10.24425/afe.2020.133352

12/4

Published quarterly as the organ of the Foundry Commission of the Polish Academy of Sciences

Impact of Ti and Fe on the Microstructure and Properties of Copper and Copper Alloys

M. Piękoś *, A. Garbacz-Klempka, J. Kozana, P.L. Żak
AGH University of Science and Technology, Faculty of Foundry Engineering,
Reymonta 23 Str., 30-059 Kraków, Poland
* Corresponding author. E-mail address: mpiekos@agh.edu.pl

Received 10.07.2020; accepted in revised form 22.10.2020

Abstract

The paper discusses issues related to the technology of melting and processing of copper alloys. An assessment was made of the impact of titanium and iron introduced in the form of pre-alloy - Ti73Fe master alloy on the microstructure and selected properties of pure copper and copper-silicon alloy. There are known examples of the use of titanium and iron additive to the copper alloy. Titanium as an additive introduced to copper alloys to improve their properties is sometimes also applicable. In the first stage of the study, a series of experimental castings were conducted with variable content of Ti73Fe master alloy entering copper in quantities of 5 %, 15 %, 25 % in relation to the mass of the metal charge. In the second stage, a silicon additive was introduced into copper in the amount of about 4 % by weight and 0.5 % and 1 % respectively of the initial Ti73Fe alloy. Thermodynamic phase parameters were modelled using CALPHAD method and Thermo-Calc software, thus obtaining the crystallization characteristics of the test alloys and the percentage of structural components at ambient temperature. Experiments confirmed the validity of the use of Ti73Fe master alloy as an additive. The pre-alloy used showed a favourable performance, both in terms of addition solubility and in the area of improvement of strength properties. Changes were achieved in the microstructure, mainly within the grain, but also in the developed dendrites of the solid solution. Changes occur with the introduction of titanium with iron into copper as well as to two-component silicon bronze.

Keywords: Copper alloys, Thermodynamic modelling, Alloying additions, Titanium, Mechanical properties, Microstructure

1. Introduction

Copper is one of the most expensive and hardly available metals. This element is characterized by several valuable properties, thanks to which it is widely used in technology. Efforts are being made to develop copper alloys by improving their properties [1-3]. This is associated with increased tensile and bending strength, improved plasticity and even their thermal resistance. Attempts are also being made to improve corrosion resistance and maintain high electrical conductivity. Such improvements can be achieved in a number of ways, e.g. by heat treatment, modification and by the introduction of appropriate alloying additives [4-7].

Copper alloys with small alloying element additions such as Ag, Be, Cd, Co, Cr, Fe, Ni, Zr, up to 5 % are called alloy copper, and above 5 % - copper alloys. They are used in industry - from chemical equipment, electronic tubular elements, solder nozzles, gas nozzles, radars and telecommunications and radio technical equipment [7,8]. Copper with iron [9-13], chrome [14-19], nickel [20-23] and titanium [24-32] are most commonly used. Copper with magnesium [33] or copper with zirconium [34] are less frequently used.

Titanium copper - the maximum solubility of titanium in copper is 8 % at 885 ^{o}C (Figure 1.). Metastable intermediate phases with an ordered structure may arise in this range before the release of the βTiCu4 equilibrium phase particles. Between the melting point of the TiCu phase particles and the eutectic transition temperature (73 % at Cu) there are peritectic reactions leading to the formation of intermetallic phases with stoichiometric formulas of Ti_3Cu_4 (57.1 at. Cu), Ti_2Cu_3 (60 at. Cu), $TiCu_2$ (66,7 at. Cu) i $TiCu_4$ (78-80.9 at. Cu) [8, 35, 36]. Cu-Ti alloys are an interesting material for foundry in the form of master alloys (pre-stops) for the correction of composition, as well as for the implementation of casting alloy modification procedures. Alloys containing CuTi10 as well as compound alloys [8, 30], among other things, are used.

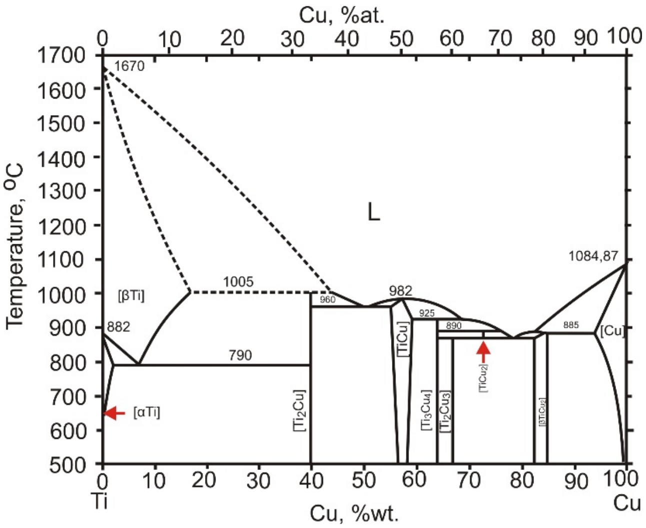

Fig. 1. Phase equilibrium diagram of Ti-Cu [8]

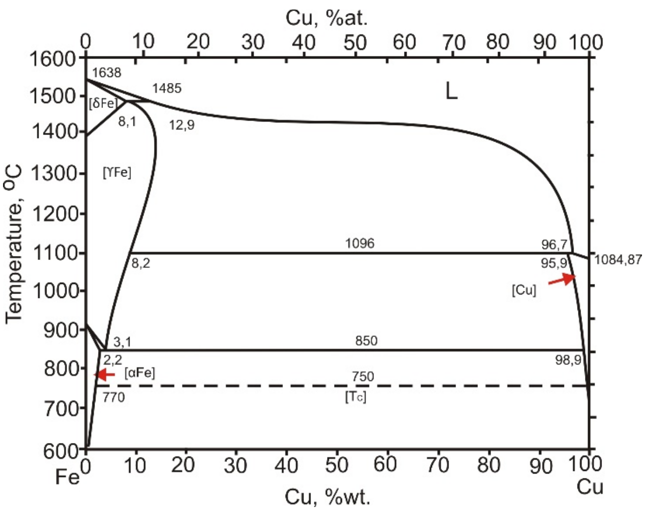

Fig. 2. Phase equilibrium diagram of Fe-Cu [8]

Iron copper – copper with small iron additives creates a very interesting and forward-looking group of materials, characterized by good performance [9]. The maximum iron solubility in copper is 4,1 wt. % at peritectic transformation temperature 1096 °C (Figure 2.) [37]. They are used to make of elastic components, enclosures for electronic devices, telecommunications equipment and measuring apparatus and other things [7, 8].

The thermodynamic analysis of the Cu-Fe-Ti system was carried out by V. Raghavan [38]. Five three-component phases are specified in this system.

Silicon bronzes with good mechanical properties, high corrosion resistance and mechanical wear. The mechanical properties of silicon bronzes depend on the amount of silicon in the alloy. As the silicon content increases, the strength and hardness of the bronzes increases and the plasticity decreases. Silicon bronzes are widely used in the production of castings such as bushings, pump housings and valve parts, rotors, plain bearings, gears [39]. They are also popular in art foundry.

A small addition of iron has a beneficial effect on the fragmentation of the structure and increase the mechanical properties. However, when the 1.5 % Fe content is exceeded in Cu-Si-Mn-Zn-Fe and 2.5 % in Cu-Si-Fe alloys, the mechanical properties of these alloys decrease. In general, in technical alloys, the iron content is between 0.5 and 1.8 %. In silicon bronzes, microstructure fragmentation can be obtained by introducing elements with a modifying effect. The most popular and effective in the fragmentation of silicon bronze microstructure is the addition of zirconium. However, there are known examples of the use of titanium additives, which also has a deoxidizing capacity. [7, 39]. The use of the Ti73Fe complex titanium-iron master alloy in the right amount should have a positive effect on the properties of the test copper and silicon alloy.

2. Investigation methodology

The work plan involved performing tests using Ti-Fe two-component master alloy to determine the impact of titanium as the main alloy reagent when introduced into copper and copper alloy with silicon. In addition, when introducing the selected TiFe master alloy, the proportion of iron in the analysed copper and silicon bronze increased. The presence of iron is sometimes referred to as contamination and is sometimes an alloying additive that acts towards grain fragmentation in Cu alloys.

In the first stage of the study, a series of experimental casting were conducted with variable content of Ti73Fe master alloy entering copper in quantities of 0 %, 5 %, 15 %, 25 % in relation to the mass of the metal charge. Obtained specimens were named with symbols Cu, CuTi4Fe, CuTi12Fe4, CuTi19Fe7 respectively.

In the second stage, a silicon additive was introduced into copper in the amount of about 4 % by weight and 0.5 % and 1 % respectively of the initial Ti73Fe alloy. Casted specimen without the Ti73Fe addition was named CuSi4 and specimens with additions: CuSi4Ti0.4 (CuSi4 + 0.5 % Ti73Fe) and CuSi4Ti0.7 (CuSi4 + 1 % Ti73Fe).

The experimental casting was carried out in an induction furnace with a chamotte-graphite crucible. The addition of Ti73Fe master alloy was introduced at a bath temperature that vary between 1100 and 1200 °C. Finished alloys were cast into metal moulds. Samples were prepared from the obtained alloys and microstructure tests were performed, tensile strength UTS, elongation A, reduction in area RA and BHN (Brinell Hardness Number) were assessed.

During the research the following was analysed: the chemical composition of the obtained alloys according to the design of experiments, using the Spectro Midex energy dispersion X-ray fluorescence spectrometer; macro- and microstructures were investigated by the NIKON SMZ 745Z and Eclipse LV 150 microscopes (OM). Samples were ruptured by means of the INSTRON device, model 1115.

Analysis of equilibrium crystallization was performed using the CALPHAD method, using the Thermo-Calc package with the TCCU copper alloy base: TCS Cu-based Alloys Database [40, 41].

2. Results of the selected tests

Samples for the chemical composition test were taken from the casting of the metal mould. The following chemical compositions of alloys summarised in Table 1 and Table 2 were obtained as a result of the tests. In the rest of the article, alloys are identified in terms of copper, titanium and iron and silicon content (column "Type of alloy").

Table 1.
Results of the chemical composition analysis of alloy Cu+Ti73Fe

No.	Type of alloy	Cu	Ti	Fe	Mo	Mn	Zn	Rest
1	Cu	99.26	0.03	0.03	0.30	0.03	0.33	0.02
2	CuTi4Fe	94.15	3.74	1.38	0.30	0.15	0.15	0.13
3	CuTi12Fe4	83.60	11.55	4.30	0.30	0.03	0.20	0.02
4	CuTi19Fe7	73.78	18.84	6.93	0.30	0.03	0.19	0.01

Table 2.
Results of the chemical composition analysis of alloy CuSi4+Ti73Fe

No.	Type of alloy	Cu	Si	Ti	Fe	Mo	Zn	Rest
5	CuSi4	95.17	4.12	0.03	0.03	0.31	0.33	0.01
6	CuSi4Ti0.4	94.78	4.10	0.37	0.13	0.28	0.31	0.03
7	CuSi4Ti0.7	94.36	4.07	0.73	0.27	0.26	0.29	0.02

Figures 3-6 show examples of characteristic images of microstructures from the first stage of testing, i.e. the assessment of the impact of variable additions of TiFe master alloy for electrolytic copper M1E.

The microstructure of pure copper used for the test process shows the dendritic structure, a bright copper solution (Cu) is visible with the separations at the boundaries of the Cu-Cu_2O aerobic eutectic grains.

The introduction of the Ti73Fe master alloy additive globally changes the microstructure of the test alloy. The master alloy has a strong deoxidizing effect. In the microstructure, the disappearance of Cu-Cu_2O eutectic is noticeable (Figures 4-6).

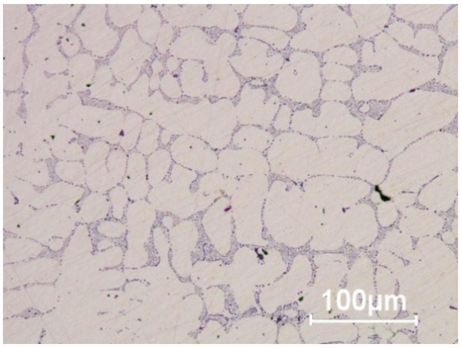

Fig. 3. Microstructure image of Cu, 200x

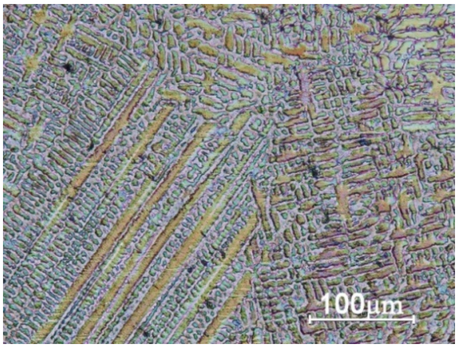

Fig. 4. Microstructure image of CuTi4Fe, 200x

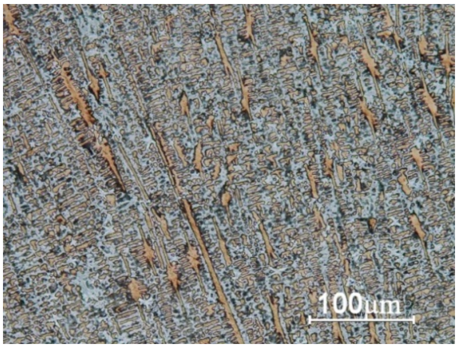

Fig. 5. Microstructure image of CuTi12Fe4, 200x

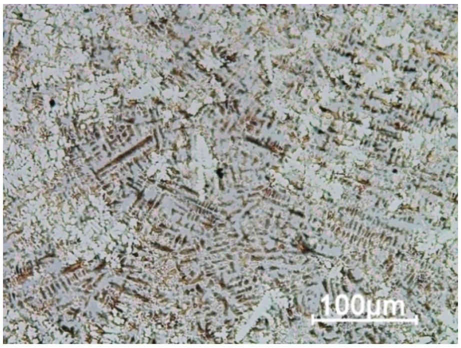

Fig. 6. Microstructure image of CuTi19Fe7, 200x

In the next stage, the CuSi4 two-component silicon bronze was introduced with a Ti-Fe master alloy in different quantities. Figures 7-9 show the microstructures of the experiment.

The CuSi4 output alloy microstructure after casting exhibits a dendritic structure - two-phase. Dendrites are formed from the α phase, and interdendritical spaces have phase γ eductins.

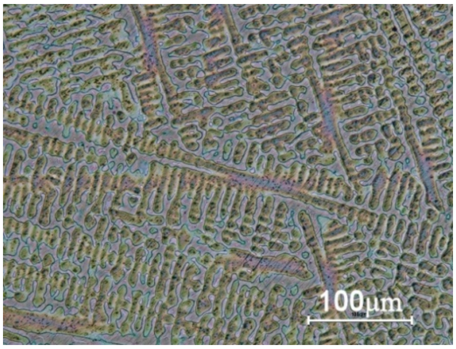

Fig. 7. Microstructure image of CuSi4, 200x

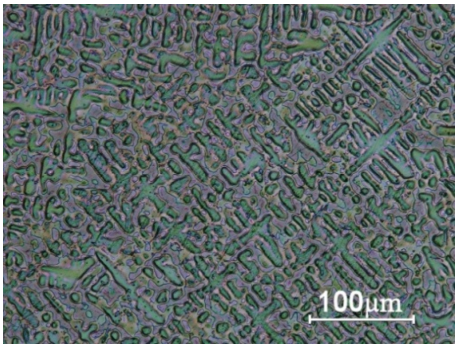

Fig. 8. Microstructure image of CuSi4Ti0.4, 200x

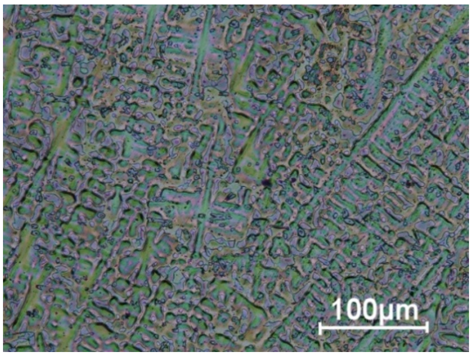

Fig. 9. Microstructure image of CuSi4Ti0.7, 200x

The resulting images of microstructures from stages one and two showed, after initial analysis, a clear effect of the additive used in both pure copper and silicon bronze. The changes are mainly related to the crystallization process in the grain area, but the morphology of detected dendrites also changes.

Visible changes in the microstructure, as a rule, cause changes in mechanical properties. The results of the tests of the obtained properties of both experiments are shown in Table 3. Individual properties are shown graphically in Figure 10 and 11.

Table 3.
Results of testing mechanical properties of samples from individual experiments

Type of alloy	UTS	Elongation A	RA	BHN
	[MPa]	%	%	-
Cu	88	9.5	4.9	32
CuTi4Fe	352	8.2	7.3	151
CuTi12Fe4	412	0.8	1.0	290
CuTi19Fe7	155	0.3	0.4	400
CuSi4	215	4.5	4.9	134
CuSi4Ti0.4	320	9.1	1.9	126
CuSi4Ti0.7	119	4.6	1.4	120

The results of the strength properties confirm the beneficial effect of titanium and iron introduced in the form of the Ti73Fe pre-alloy. The applied additive significantly increased the hardness and tensile strength of the alloy. The maximum strength was achieved with 15 % of the master alloy additive, which represented 11.55 % and 4.3 % of the Ti and Fe content of the alloy (CuTi12Fe4). However, the lower titanium and iron content of 3.7 % and 1.3 % (CuTi4Fe) in the alloy, respectively, makes the resulting material more favourable.

The properties of the CuSi4 silicon copper are improved after the addition of 0.5 % Ti73Fe master alloy, representing 0.4 % titanium and 0.1 % iron alloy content (CuSi4Ti0.4). A larger addition of titanium has resulted in a deterioration of all the strength properties of the alloy. The observed dependencies are shown in Figures 10 and 11.

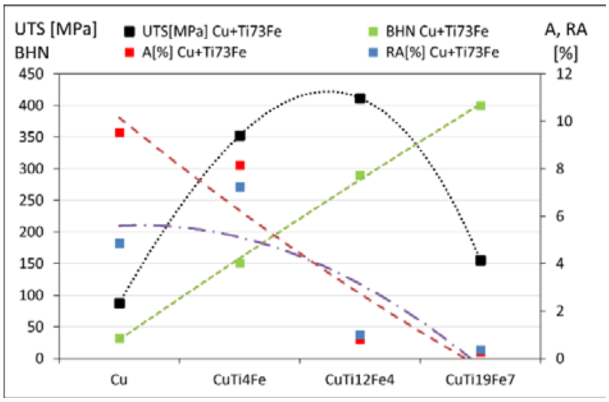

Fig. 10. Graphical listing of the mechanical properties results of samples from individual experiments Cu+Ti73Fe

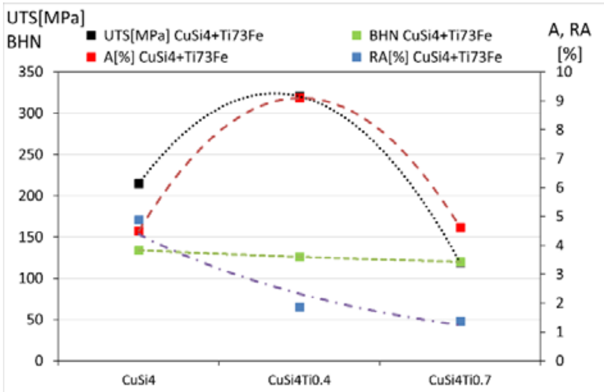

Fig. 11. Graphical listing of the mechanical properties results of samples from individual experiments CuSi4+Ti73Fe

4. CALPHAD thermodynamic modelling

The microstructure analysis was verified based on the results of CALPHAD calculations. CALPHAD alloy modelling using Thermo-Calc software was performed for alloys obtained in the experiment. A simulation of the alloy cooling process was simulated taking into account phase changes under equilibrium conditions. In addition, modelling for alloy 11 (Cu-O for oxygen content 0.5 %) was carried out. In the case of alloy 1 (Cu) with few impurities such as Ti, Fe, Mo, Mn, Zn, the presence of 0,5 % aerobic eutectic Cu-Cu_2O was observed in the microstructure, which was included in the Thermo-Calc modelling.

Modelling graphs of the theoretical crystallization of the test alloys were obtained. An example of a CuTi12Fe4 alloy cooling simulation graph is shown in Figure 12. Temperatures T1 and T2 are the temperatures at which under assumption of thermodynamic equilibrium conditions it is possible nucleation and growth of successive phases from liquid and at temperatures T3 and T4 in the solid state. At T3 temperature, we observe the end of the crystallization – no more LIQUID phase is present below this temperature. The T5 temperature can be taken as the ambient temperature.

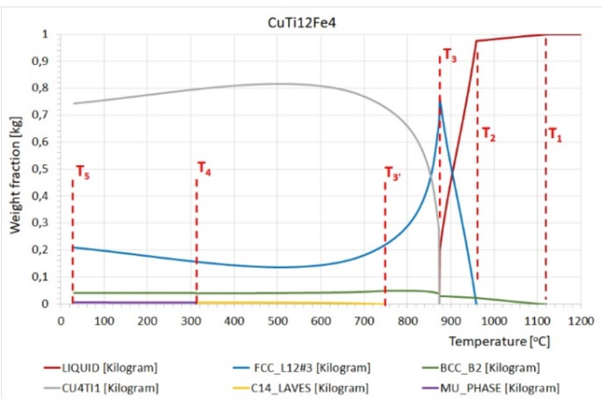

Fig. 12. Simulation of the crystallization of alloy 3 with marked characteristic transformation temperatures.

Table 4.
Results of characteristic copper phase change temperatures with TiFe additives modelled using Thermo-Calc

Sample	T_1 [°C]	T_2 [°C]	T_3 [°C]	T_4 [°C]	T_5 [°C]	Weight fraction in 30°C	Weight percent of element in phase							
11 (Cu-CuO)														
LIQUID [Kg]		1082	1066											
FCC_L12 [Kg]		1082	1066		30	0,9955	Cu	100,00						
CUPRITE_C3 [Kg]			1066		30	0,0045	Cu	88,8190	O	11,1810				
1 (Cu)														
LIQUID [Kg]	1230		1062											
FCC_L12 [Kg]		1080	1066		30	0,9903	Cu	99,6673	Zn	0,3029	Mn	0,0298		
CUPRITE_C3 [Kg]			1063		30	0,0045	Cu	88,8190	O	11,1810				
BCC_B2 [Kg]	1230				30	0,0026	Mo	99,7942	Mn	0,2056	Ti	0,0002		
CU4TI1 [Kg]				276	30	0,0019	Cu	84,4781	Ti	15,5219				
MU_PHASE [Kg]				530	30	0,0007	Mo	59,5515	Fe	40,4039				
2 (CuTi4Fe)														
LIQUID [Kg]	1185		952											
FCC_L12 [Kg]		1044	786		30	0,7423	Cu	99,5970	Zn	0,20208	Mn	0,2009	Ti	0,00002
C14_LAVES [Kg]			771	311										
BCC_B2 [Kg]	1085		923											
BCC_B2#3 [Kg]			815		30	0,0118	Fe	99,9226	Mn	0,0770	Mo	0,0004		
CU4TI1 [Kg]			786		30	0,2409	Cu	84,4766	Ti	15,5234				
MU_PHASE [Kg]	1051-1038		955-771		311-30	0,0050	Mo	59,5522	Fe	40,4237	Cu	0,0241		
3 (CuTi12Fe4)														
LIQUID [Kg]	1120		872											
FCC_L12 [Kg]		958	872		30	0,2103	Cu	98,9177	Zn	0,9508	Mn	0,1315	Ti	0,00013
C14_LAVES [Kg]			746	311										
BCC_B2 [Kg]	1120		872		30	0,0410	Fe	99,9426	Mo	0,00038	Mn	0,057		
CU4TI1 [Kg]			873		30	0,7436	Cu	84,4680	Ti	15,5320				
MU_PHASE [Kg]				311	30	0,0050	Mo	59,5522	Fe	40,4238	Cu	0,0239		
4 (CuTi19Fe7)														
LIQUID [Kg]	1130		850											
FCC_L12 [Kg]			850		30	0,0069	Cu	75,1659	Zn	24,8171	Mn	0,0168	Ti	0,00024
C14_LAVES [Kg]			665	316										
BCC_B2 [Kg]	1130	873/862			30	0,0674	Fe	99,7974	Mo	0,00039	Mn	0,2015	Ti	0,00069
CU4TI1 [Kg]		873			30	0,6779	Cu	84,1568	Ti	15,8432				
CU3TI2 [Kg]		862			30	0,2423	Cu	66,5640	Ti	33,4360				
MU_PHASE [Kg]				316	30	0,0050	Mo	59,5532	Fe	40,4359	Cu	0,0109		
CUMNZN [Kg]				59	30	0,0005	Cu	34,6293	Zn	35,522	Mn	29,849		

Crystallizing pure copper should solidify at a constant temperature of 1084.84 °C (TC 1082 °C – FCC_L12). Small amount of dissolved oxygen in copper (0.5 %) will cause the appearance at 1066 °C of the so-called aerobic CUPRITE_C3 eutectic.

Introducing titanium together with iron in the Ti73Fe master alloy into copper: titanium mainly secretes in phases with Cu_4Ti and Cu_3Ti_2 copper, and iron mainly for BCC_B2, BCC_B#3 and MU_PHASE. The FCC_L12 phase is mainly copper and small separation of other alloying components, a similar situation occurs in phases of type BCC. The exact compositions of each phase are shown in Table 4.

The results of the participation of the individual phases at 30 °C are graphically presented (Figure 13).

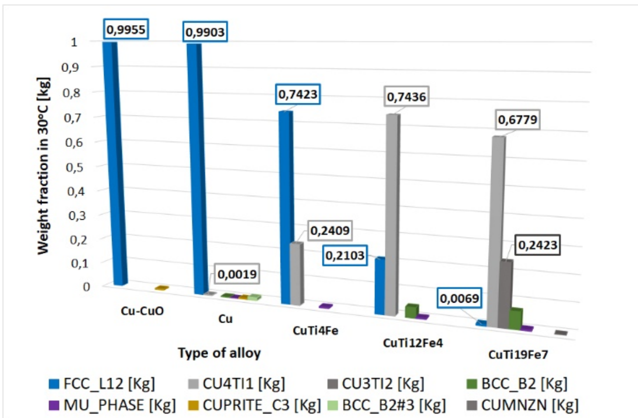

Fig. 13. Weight fraction of copper phases with TiFe additives at 30 °C modelled using Thermo-Calc

Modelling for CuSi4 alloy is as follows (Table 5): at ambient temperature, the main structural components are FCC_L12 solution (Cu 97.6 wt. %, Si 1.9 wt. %, Zn 0.4 wt. %) and phase $Cu_{56}Si_{11}$_GAMMA (with a composition of Cu91.9Si7.9Zn0.1). A small addition of titanium induces an increasing phase share of Cu_4Ti (Cu84.4Ti15.6) and iron- phase $FeSi_2$_L. Graphically, the mass participation of phases modelled with the Thermo-Calc CuSi4 alloy program with TiFe additives at 30 °C is shown in Figure 14.

Table 5.
Results of characteristic phase transformation temperatures of CuSi4 alloy modelled using Thermo-Calc

Sample	T_1 [°C]	T_2 [°C]	T_3 [°C]	T_4 [°C]	T_5 [°C]	Weight fraction in 30°C	Weight percent of element in phase							
5 (CuSi4)														
LIQUID [Kg]	1227	984	906											
FCC_L12 [Kg]		984		470	30	0,6370	Cu	97,6142	Si	1,9387	Zn	0,4471	Ti	0,00002
BCC_B2 [Kg]	1227				30	0,0031	Mo	99,9997	Ti	0,0003				
CU56SI11_GAMMA [Kg]				470	30	0,3574	Cu	91,8859	Si	7,9877	Zn	0,1264		
CU4TI1 [Kg]				276	30	0,0019	Cu	84,3783	Ti	15,6217				
FESI_B20 [Kg]			791	155										
FESI2_L [Kg]				155	30	0,0006	Si	50,1442	Fe	49,8558				
6 (CuSi4Ti0.4)														
LIQUID [Kg]	1205		893											
FCC_L12 [Kg]		980	893		30	0,6259	Cu	97,6328	Si	1,9387	Zn	0,4285	Ti	0,00002
BCC_B2 [Kg]	1205				30	0,0028	Mo	99,9997	Ti	0,0003				
CU56SI11_GAMMA [Kg]				448	30	0,3450	Cu	91,8911	Si	7,9877	Zn	0,1212		
CU4TI1 [Kg]				440	30	0,0237	Cu	84,3785	Ti	15,6215				
FESI_B20 [Kg]		911		155										
FESI2_L [Kg]				155	30	0,0026	Si	50,1442	Fe	49,8558				
7 (CuSi4Ti0.7)														
LIQUID [Kg]	1188	975	882											
FCC_L12 [Kg]		975			30	0,6203	Cu	97,6541	Si	1,9387	Zn	0,4072	Ti	0,00002
BCC_B2 [Kg]	1188				30	0,0026	Mo	99,9997	Ti	0,0003				
CU56SI11_GAMMA [Kg]				447	30	0,3250	Cu	91,8971	Si	7,9877	Zn	0,1152		
CU4TI1 [Kg]				465	30	0,0467	Cu	84,3788	Ti	15,6212				
FESI_B20 [Kg]		953		155										
FESI2_L [Kg]				155	30	0,0054	Si	50,1442	Fe	49,8558				
CU3TI2 [Kg]			518	458										

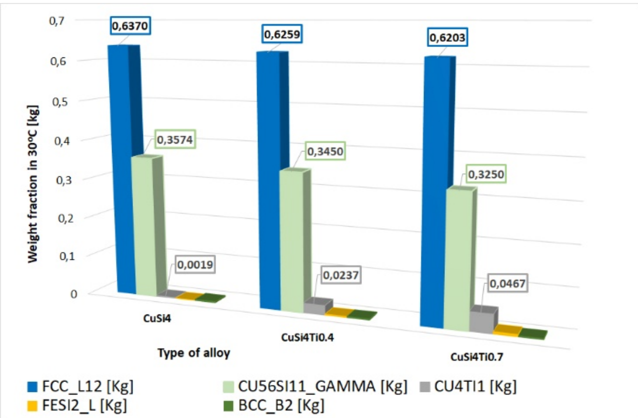

Fig. 14. Weight fraction of CuSi4 alloy phases with TiFe additives at 30 °C modelled using Thermo-Calc

5. Conclusions

The CALPHAD method simulates the cooling and crystallization processes of the test alloys. This allows you to identify the phases responsible for the individual properties of the test alloys. The experimental process of the experiment, i.e. images of microstructures and the resulting characteristics of strength properties gain additional confirmation by determining the theoretical participation of the individual structural components. The tool in the form of Thermo-Calc software allows to obtain detailed data, obtained experimentally only by means of phase identification by analytical methods (XRD, SEM-EDS, EBSD).

Analyzing the effects of titanium together with the iron introduced into pure copper, we observe the following changes. The FCC_L12 phase practically reads copper is characterized by relatively small properties. The introduction of the Ti73Fe triggered the appearance of Cu_3Ti_2 phase hard separations in the microstructure (Ti value at a rate above 11.55 %) which caused a sharp increase in hardness, at the expense of a decrease in the strength of the alloy – a visible degradation of the beneficial microstructure. Titanium in the amount of 3.7 and 11.55 % has a positive effect in copper, causing crystallization of the Cu_4Ti phase in the amount of 0.2 and 0.7 % respectively at the expense of depletion of the FCC_L12. This results in a high tensile strength alloy with suitably high plasticity or high hardness. The impact of Ti and Fe was graphically demonstrated in the form of a mass phase share combination with selected properties of UTS, BHN for subsequent copper alloys: CuTi4Fe, CuTi12Fe4, CuTi19Fe7 (Figure 15).

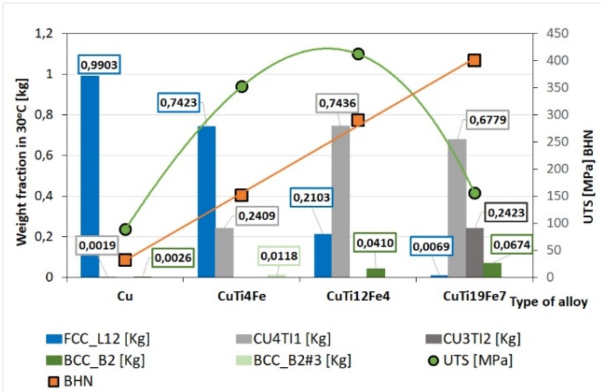

Fig. 15. Weight fraction of phases with selected copper properties with TiFe additives (UTS, BHN)

The tests carried out on CuSi4 allow the following conclusions to be obtained. Introducing titanium and iron in the Ti73Fe master alloy, the main impact is evident through the appearance of the Cu_4Ti phase. The addition of titanium in the amount of 0.4 % resulted in the separation of the Cu_4Ti phase in the amount of 0.02 %, causing the desired formation of the components of the microstructure, which resulted in an increase in tensile strength and plasticity with a slight decrease in the hardness of the alloy. Above this value, beneficial separations of structural components are degraded, resulting in a decrease in the mechanical properties of CuSi4. The influence of Ti and Fe in copper with silicon is shown graphically in the form of a juxtaposition of phase mass participation with selected properties of UTS, BHN for subsequent copper alloys: CuSi4, CuSi4Ti0.4, CuSi4Ti0.7 (Figure 16).

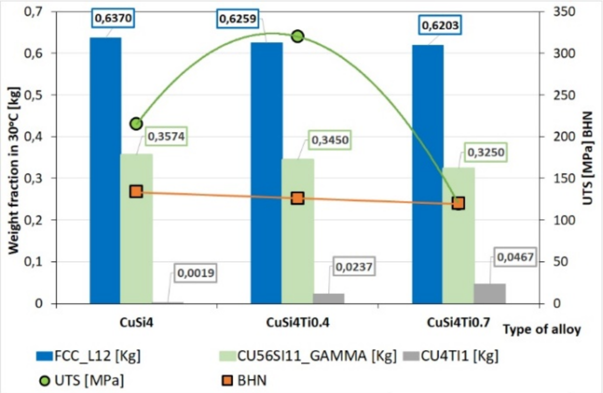

Fig. 16. Weight phase share with selected CuSi4 alloy properties (UTS, BHN)

The metallographic tests carried out and the results obtained from selected mechanical properties of the analysed alloys demonstrated the validity of the studies undertaken. Changes were achieved in the microstructure, mainly within the grain, but also in the developed dendrites of the solid solution. Changes occur with the introduction of titanium with iron into copper as well as to two-component silicon bronze.

The pre-alloy used showed a favourable performance, both in terms of master alloy solubility and in the area of improvement of strength properties. Experiments confirmed the validity of the use of Ti73Fe master alloy as an additive. Titanium in this form is easily introduced into pure copper as well as copper alloy with silicon causing changes in the properties of the test alloys.

References

[1] Rzadkosz, S., Garbacz-Klempka, A., Kozana, J., Piękoś, M. & Kranc, M. (2014). Structure and properties research of casts made with copper alloys matrix. *Archives of Metallurgy and Materials*. 59(2), 775-778.

[2] Rzadkosz, S., Kranc, M., Garbacz-Klempka, A., Kozana, J. & Piękoś, M. (2015). Refining Processes in the Copper Casting Technology. *Metalurgija*. 54(1), 259-262.

[3] Rzadkosz, S., Kranc, M., Garbacz-Klempka, A., Piękoś, M., Kozana, J. & Cieślak, W. (2014). Research on technology of alloyed copper casting. *Archives of Foundry Engineering*. 14(2), 79-84.

[4] Eze, A.A., Jamiru, T., Sadiku, E.R., Durowoju, M.O., Kupolati, W.K., Ibrahim, I.D., Obadele, B.A., Olubambi, P.A. & Diouf, S. (2018). Effect of titanium addition on the microstructure, electrical conductivity and mechanical properties of copper by using SPS for the preparation of Cu-Ti alloys. *Journal of Alloys and Compounds*. 736, 163-171. DOI:10.1016/j.jallcom. 2017.11.129.

[5] Takahashi, T., Hashimoto, Y. & Koyama, K. (1989). Effect of Ti and Zr Additions on the Internal Oxidation of Cu–Si Alloy. *Materials Transactions, JIM*. 30(2), 127-136. DOI:10.2320/matertrans1989.30.127.

[6] Polok-Rubiniec; M., Konieczny; J., Labisz, K. & Włodarczyk-Fligier, A., (2016). Microstructure and Service Properties of Copper Alloys. *Archives of Metallurgy and Materials*. 61(3), 1277-1282. DOI:10.1515/amm-2016-0211.

[7] Rzadkosz, S. (2013). *Foundry of copper and copper alloys* (Odlewnictwo miedzi i jej stopów). Kraków: Wydawnictwo Naukowe Akapit. (in Polish).

[8] Rdzawski, Z. (2009). *Alloy copper*. (Miedź stopowa), Gliwice: Wydawnictwo Politechniki Śląskiej. (in Polish).

[9] Rdzawski, Z.M., Stobrawa, J. & Głuchowski, W. (2009) Structure and properties of CuFe2 alloy. Journal of *Achievements in Materials and Manufacturing Engineering*. 33(1), 7-18.

[10] Kim, H.G., Han, S.Z., Euh, K. & Lim, S.H. (2011). Effects of C addition and thermo-mechanical treatments on microstructures and properties of Cu–Fe–P alloys. *Materials Science and Engineering: A*. 530, 652-658. DOI: 10.1016/j.msea.2011.10.041.

[11] Dong, Q.Y., Shen, L.N., Cao, F., Jia, Y.L., Liao, K.L.& Wan g, M.P. (2015) Effect of thermomechanical processing on the microstructure and properties of a Cu–Fe–P alloy. *Journal of Materials Engineering and Performance*. 24, 1531-1539. DOI: 10.1007/s11665-014-1352-6.

[12] Fernee, H., Nairn, J. & Atrens, A. (2001) Precipitation hardening of Cu-Fe-Cr alloys part I Mechanical and electrical properties. *Journal of Materials Science*. 36, 2711-2719. DOI: 10.1023/A:1017916930459.

[13] Lu, D.P., Wang, J., Zeng, W.J., Liu, Y., Lu, L. & Sun, B.D. (2006). Study on high-strength and high-conductivity Cu–Fe–P alloys. *Materials Science and Engineering: A*. 21, 254-259. DOI: 10.1016/j.msea.2006.01.068.

[14] Stobrawa, J., Ciura, L. & Rdzawski, Z. (1996). Rapidly solidified strips of Cu-Cr alloys. *Scripta Materialia*. 34(11), 1759-1763. DOI:10.1016/1359-6462(96)00053-X.

[15] Pang, Y., Xia, C., Wang, M., Li, Z., Xiao, Z. & Wie, H. (2014). Effects of Zr and (Ni, Si) additions on properties and microstructure of Cu–Cr alloy. *Journal of Alloys and Compounds*. 582, 786-792. DOI: 10.1016/j.jallcom. 2013.08.146.

[16] Dobatkin, S.V., Gubicza, J., Shangina, D.V., Bochvar, N.R. & Tabachkova, N.Y. (2015). High strength and good electrical conductivity in Cu–Cr alloys processed by severe plastic deformation, *Materials Letters*. 153, 5-9. DOI: 10.1016/j.matlet. 2015.03.144.

[17] Batra, I.S., Dey, G.K., Kulkarni, U.D. & Banerjee, S. (2003). Precipitation in a Cu–Cr–Zr alloy. *Materials Science and Engineering: A*, 356(1-2), 32-36. DOI: 10.1016/S0921-5093(02)00852-3.

[18] Liu, Y., Li, Z., Jiang, Y., Zhang, Y., Zhou, Z., & Lei, Q. (2017). The microstructure evolution and properties of a Cu–Cr–Ag alloy during thermal-mechanical treatment. *Journal of Materials Research*. 32(7), 1324-1332. DOI: 10.1557/jmr. 2017.17.

[19] Kermajani, M., Raygan, Sh., Hanayi, K. & Ghaffari, H. (2013). Influence of thermomechanical treatment on microstructure and properties of electroslag remelted Cu–Cr–Zr alloy. *Materials & Design*. 51, 688-694. DOI: 10.1016/j.matdes.2013.04.062.

[20] Srikanth, S. & Jacob, K.T. (1989). Thermodynamic properties of Cu–Ni alloys: measurements and assessment. *Materials*

Science and Technology. 5(5), 427-434, DOI: 10.1179/mst.1989.5.5.427.

[21] Straumal, B.B., Protasova, S.G., Mazilkin, A.A., Rabkin, E., Goll, D., Schütz, G., Baretzky, B. & Valiev, RZ. (2012). Deformation-driven formation of equilibrium phases in the Cu-Ni alloys. *Journal of Materials Science*. 47, 360-367. DOI: 10.1007/s10853-011-5805-0.

[22] Mathiyarasu, J., Palaniswamy, N. & Muralidharan, V. (2000). Corrosion Resistance of Cuupronickels – An Overview. *Corrosion Reviews*. 18(1), 2000, 65-103. DOI: 10.1515/ corrrev.2000.18.1.65.

[23] Taher, A. (2015). Corrosion Behavior of Copper-Nickel Alloy in Marine Environment (Review Paper). *Applied Mechanics and Materials*. 799-800, 222-231. DOI: 10.4028/www.scientific.net/ AMM.799-800.222.

[24] Nagarjuna, S., Srinivas, M., Balasubramanian, K., & Sarma, D.S. (1999). On the variation of mechanical properties with solute content in Cu–Ti alloys. *Materials Science and Engineering: A*, 259(1), 34-42. DOI: 10.1016/S0921-5093(98)00882-X.

[25] Nagarjuna, S., Balasubramanian, K., & Sarma, D.S. (1999). Effect of prior cold work on mechanical properties, electrical conductivity and microstructure of aged Cu-Ti alloys. *Journal of materials science*, 34(12), 2929-2942. DOI: 10.1023/ A:1004603906359.

[26] Suzuki, S., Hirabayashi, K., Shibata, H., Mimura, K., Isshiki, M. & Waseda, Y. (2003) Electrical and thermal conductivities in quenched and aged high-purity Cu–Ti alloys. *Scripta Materialia*. 48(4), 431-435. DOI: 10.1016/S1359-6462(02)00441-4.

[27] Soffa, W.A., & Laughlin, D.E. (2004). Highstrength age hardening copper–titanium alloys: redivivus. *Progress in Materials Science*. 49(3-4), 347-366. DOI: 10.1016/S0079-6425(03)00029-X.

[28] Semboshi, S., & Konno, T.J. (2008). Effect of aging in hydrogen atmosphere on electrical conductivity of Cu–3at.% Ti alloy. *Journal of Materials Research*, 23(2), 473-477. DOI: 10.1557/jmr.2008.0050.

[29] Semboshi, S., & Takasugi, T. (2013). Fabrication of high-strength and high-conductivity Cu–Ti alloy wire by aging in a hydrogen atmosphere. Journal of Alloys and Compounds, 580, S397-S400.

[30] Kurdewan, T., Zilly, A. (2019). Copper alloys with titanium - Mechanisms of action of low alloy contents in materials with high strength and good conductivity (Kupferlegierungen mit Titan - Wirkmechanismen geringer Legierungsanteile in Werkstoffen mit hoher Festigkeit und guter Leitfähigkeit). *Metall*. 11, 436-439. (in German).

[31] Vorotilo, S., Loginov, P.A., Kovalev, D.Yu. & Levashov, E.A. (2020). DFT – Driven design of hierarchically structured, strong and highly conductive alloys in Cu–Ti system via in situ hydration - re-oxidation. Journal of Alloys and Compounds. 832, 154823. DOI: 10.1016/j.jallcom.2020.154823.

[32] Wei, H., Dai, X., Han, P., Wei, Y. & Hou, L. (2020). Surface mechanical attrition treatment-induced dissolution of Cu_4Ti precipitates in Cu–4wt-%Ti alloy. *Materials Science and Technology*. 36(6), 661-667. DOI: 10.1080/02670836.2020. 1726600.

[33] Kranc, M., Sikora, G., Górny, M. & Garbacz-Klempka, A. (2017) The Influence of Mg Additive on the Structure and Electrical Conductivity of Pure Copper Castings. Archives of Foundry Engineering. 17(4), 85-90. DOI: 10.1515/afe-2017-0135.

[34] Arnberg, L, Backmark, U., Bäckström, N. & Lange, J. (1986). A new high strength, high conductivity Cu-0.5wt.%Zr alloy produced by rapid solidification technology. Materials Science and Engineering. 83(1), 115-121. DOI:10.1016/0025-5416(86)90178-3.

[35] Kumar, K.C., Ansara, I., Wollants, P. & Delaey L. (1996). Thermodynamic Optimization of the Cu-Ti System. *Zeitschrift fur metallkunde*. 87(8), 666-672.

[36] Dumitrescu, L.F.S., Hillert, M. & Saunders N. (1998). Comparison of Fe-Ti Assessments. *Journal of phase equilibria*. 19(5), 441-48. DOI: 10.1361/ 105497198770341923.

[37] Swartzendruber, L.J. (1993) Cu-Fe (Copper-Iron). *Phase Diagrams of Binary Iron Alloys*. ASM International, Materials Park, 131-37.

[38] Raghavan, V. (2002). Cu-Fe-Ti (Copper-Iron-Titanium). *Journal of Phase Equilibria*. 23, 172 DOI: 10.1361/1054971023604152.

[39] Garbacz-Klempka, A., Kozana, J., Piękoś, M., Papaj, M., Papaj, P. & Perek-Nowak M. (2018). Influence of modification in centrifugal casting on microstructure and mechanical properties of silicon bronzes. *Archives of Foundry Engineering*. 18(3), 11-18. DOI: 10.24425/123594.

[40] Wróbel, M. & Burbelko, A. (2015). CALPHAD method - a modern technique for obtaining thermodynamic data (Metoda CALPHAD – nowoczesna technika pozyskiwania danych termodynamicznych). *Archives of Foundry Engineering*. 14(spec.3). 79-84 (in Polish).

[41] Wang, C., Huang, F., Lu, Y., Yang, S., Yang, M. & Liu, X. (2013). Experimental Investigation and Thermodynamic Calculation, *Journal of ELECTRONIC MATERIALS*. 42(10), 2961-2974. DOI: 10.1007/s11664-013-2695-8